

Supporting Information

Ambient Blade Coating of Mixed Cation, Mixed Halide Perovskites without Drip: *In Situ* Investigation and Highly Efficient Solar Cells

Ming-Chun Tang^{a†}, Yuanyuan Fan^{b†}, Dounya Barrit^a, Xiaoming Chang^b, Hoang Dang^c, Ruipeng Li^d, Kai Wang^a, Detlef-M. Smilgies^e, Shengzhong (Frank) Liu^b, Stefaan De Wolf^a, Thomas D. Anthopoulos^{a*}, Kui Zhao^{b*}, and Aram Amassian^{a,c*}

^aKing Abdullah University of Science and Technology (KAUST), KAUST Solar Center (KSC), and Physical Science and Engineering Division (PSE), Thuwal, 23955-6900, Saudi Arabia.

^bKey Laboratory of Applied Surface and Colloid Chemistry, National Ministry of Education, Shaanxi Key Laboratory for Advanced Energy Devices, and Shaanxi Engineering Lab for Advanced Energy Technology, School of Materials Science and Engineering, Shaanxi Normal University, Xi'an 710119, China.

^cDepartment of Materials Science and Engineering, North Carolina State University, Raleigh, NC, 27695, USA.

^dNSLS-II, Brookhaven National Laboratory (BNL), Upton, NY 11973, USA.

^eCornell High Energy Synchrotron Source (CHESS), Cornell University, Ithaca, NY 14850, USA

Experimental Section

Materials, lead halide precursor solutions, and deposition protocol

Materials: Lead iodide (PbI_2 , 99.99 %) was purchased from Alfa Aesar. Lead (II) bromide (PbBr_2 , 99.99 %), cesium iodide (CsI , 99.9 %), methylammonium bromide (MABr , 98 %), formamidinium iodide (FAI , 99.5 %) were purchased from p-OLED. Dimethyl sulfoxide (DMSO , 99.9 %) and N,N -dimethylformamide (DMF , 99.8 %) were purchased from Sigma-Aldrich.

Device fabrication: The perovskite precursor solution preparation was conducted under an inert atmosphere inside a nitrogen glove box. The precursor solution (1.2 M) was prepared with FAI , MABr , PbI_2 , PbBr_2 , and CsI dissolved in a dimethyl sulfoxide (DMSO) and N,N -dimethylformamide (DMF) (volume ratio of 4:1) in a glovebox. For example, the $\text{Cs}_{0.05}\text{FA}_{0.8}\text{MA}_{0.15}\text{PbI}_{2.55}\text{Br}_{0.45}$ precursor solution (1.2 M) was prepared with FAI (0.96 M), MABr (0.18 M), PbI_2 (1.014 M), PbBr_2 (0.186 M), and CsI (0.06 M) dissolved in a mixture of DMSO and DMF (4:1 v/v) for blade coating. The Spiro-OMeTAD solution was prepared by dissolving 90 mg spiro-OMeTAD, 18 μL lithium bis(trifluoromethanesulfonyl) imide (99 %, Acros Organics, 520 mg mL^{-1}) in acetonitrile (99.7 %, Alfa Aesar), 30 μL cobalt dopant (Co TFSI salt, Anhydrous ACN Sigma Aldrich, the dopant solution should be 300 mg cobalt 3 in 1 ml CAN), and 30 μL 4-tert-butylpyridine (96 %, Aldrich) in 1 mL chlorobenzene (99.8 %, Aldrich). All these solutions were prepared under inert atmosphere inside a nitrogen glove box. The FTO-coated glass (2.8 cm \times 2.8cm) was cleaned by sequential sonication in acetone, isopropanol and ethanol for 30 min each and then dried under N_2 flow and treated by O_3 plasma for 17 min. The TiO_2 was prepared by chemical bath deposition with the clean substrate immersed in a TiCl_4 (CP, Sinopharm Chemical Reagent Co., Ltd) aqueous solution with the volume ratio of $\text{TiCl}_4:\text{H}_2\text{O}$ equal to 9:400 at 70 $^\circ\text{C}$ for 1 hour, its thickness is around 65 nm.^{1,2} The perovskite precursor solution (6 μL) was blade-coated onto the substrate with a coating speed of 1000 mm/min and the blade gap of 15 μm at 150 $^\circ\text{C}$, followed by annealing at 100 $^\circ\text{C}$ for 10 min in air. Subsequently, the hole-transporting layer was deposited on top of the perovskite layer by spin coating Spiro-OMeTAD solution at 5000 rpm for 30 s in ambient air followed by vacuum evaporation of 100 nm gold electrode on the top of the cell.

Characterization

Grazing Incidence Wide Angle X-ray Scattering (GIWAXS)

All experiments were conducted at Cornell High Energy Synchrotron Source (CHESS) at D1 beamline. A 0.5×0.1 mm monochromated X-ray beam (double-bounce multilayer monochromator) with a wavelength of 1.16 \AA (10.6 keV) was used. Mathematically, $q = 4\pi\sin\theta/\lambda$, where θ denotes total scattering angle multiplied by 0.5 and λ is the wavelength of the x-ray used for measurement. The wavelength of the beam was 0.1166 nm. GIWAXS data were collected with a Pilatus 200k pixel array detector (Dectris, Baden-Dattwil, Switzerland; 100 frames per second) placed at 170.96 mm away from the sample and each blade-coating process was continuously recorded with the frame rate of 5 images/s. The incidence angle was kept at 0.5 degree and glass substrate ($2.8 \text{ cm} \times 2.8 \text{ cm}$) with TiO_2 coated was utilized during GIWAXS measurements. All the GIWAXS measurements were performed in an ambient environment where relative humidity was around 20–25 %. *In situ* GIWAXS measurements were conducted during blade coating using a custom-built setup. Each sample for blade coating was aligned at the same temperature used for coating. The blade coating speed was computer-controlled remotely outside the hutch. Other parameters such as blade angle and distance between blade and sample were managed manually. There was a delay of around 20 seconds between solution dropping and the start of blade coating/ measurement.

Optical metrology

UV-Visible absorption spectra were acquired on a PerkinElmer UV-Lambda 950 instrument.

Electronic microscopy

The surface morphology of the perovskite films was characterized by SEM (FE-SEM; SU-8020, Hitachi).

X-ray diffraction (XRD)

XRD measurements were carried out in a θ - 2θ configuration with a scanning interval of 2θ between 10° and 60° on a Rigaku Smart Lab (X-ray Source: Cu $K\alpha$; $\lambda = 1.54 \text{ \AA}$). Scan speed is $5^\circ/\text{minute}$.

Solar cell characterizations

The J - V performance of the perovskites solar cells was analyzed by Keithley 2400 source under an ambient air condition at room temperature, and the illumination intensity was 100 mW cm^{-2} (AM 1.5G Oriel solar simulator). The scan rate was 0.1 V s^{-1} . The delay time was 10 ms and the scan step was 0.02 V. The device testing voltage range was -0.1V to 1.2V. The power output of the lamp was calibrated by an NREL-traceable KG5 filtered silicon reference cell. A metal aperture to avoiding light scattering from the metal electrode into the device during the measurement defines the device area of 0.09 cm^2 .

Mobility measurement

Electron-only devices (FTO/ c-TiO₂/ perovskites/ PCBM/ Ag) were fabricated to calculate the electron mobility of the devices. The dark J - V characteristics of the electron-only devices were measured by a Keithley 2400 source. The mobility is extracted by fitting the J - V curves using the

Child's law given by $J = \frac{9}{8} \epsilon_0 \epsilon_r \mu_{SCL} \frac{V^2}{d^3}$, where J is the current density, V is the applied voltage, ϵ_0 is the vacuum permittivity, ϵ_r is the relative dielectric constant, and d is the thickness of the film.³

The trap state density was determined by the trap-filled limit voltage using the equation:

$N_t = \frac{2\epsilon_0 \epsilon_r V_{TFL}}{qL^2}$, where ϵ_0 is the vacuum permittivity, ϵ_r is the relative dielectric constant, V_{TFL} is the onset voltage of the trap-filled limit region, q is the elemental charge, and L is the thickness of the film.⁴

Supporting Data

Perovskites	V_{oc} (V)	J_{sc} (mA/cm ²)	FF (%)	PCE (%)
FAPbI ₃	0.98 (0.97 ± 0.01)	20.46 (20.86 ± 0.82)	61.60 (60.63 ± 1.87)	12.35 (9.03 ± 2.44)
FAPbI _{2.55} Br _{0.45}	1.03 (0.95 ± 0.05)	20.90 (21.39 ± 0.95)	64.21 (59.04 ± 3.33)	13.85 (11.64 ± 0.89)
FA _{0.85} MA _{0.15} PbI _{2.55} Br _{0.45}	1.00 (0.97 ± 0.02)	22.86 (21.63 ± 1.00)	69.11 (66.20 ± 1.30)	15.80 (13.89 ± 0.84)
FA _{0.8} MA _{0.15} Cs _{0.05} PbI _{2.55} Br _{0.45}	1.09 (1.01 ± 0.03)	22.50 (22.85 ± 0.53)	74.23 (71.00 ± 3.16)	18.20 (16.40 ± 1.22)
FA _{0.8} MA _{0.15} Cs _{0.05} PbI ₃	1.03 (0.97 ± 0.02)	22.74 (22.54 ± 0.64)	69.38 (66.04 ± 2.31)	16.25 (14.10 ± 0.83)

Table S1. PV parameters of the blade-coated 3D hybrid perovskite solar cells with best and average values (FAPbI₃, FAPbI_{2.55}Br_{0.45}, FA_{0.85}MA_{0.15}PbI_{2.55}Br_{0.45}, FA_{0.8}MA_{0.15}Cs_{0.05}PbI_{2.55}Br_{0.45}, and FA_{0.8}MA_{0.15}Cs_{0.05}PbI₃).

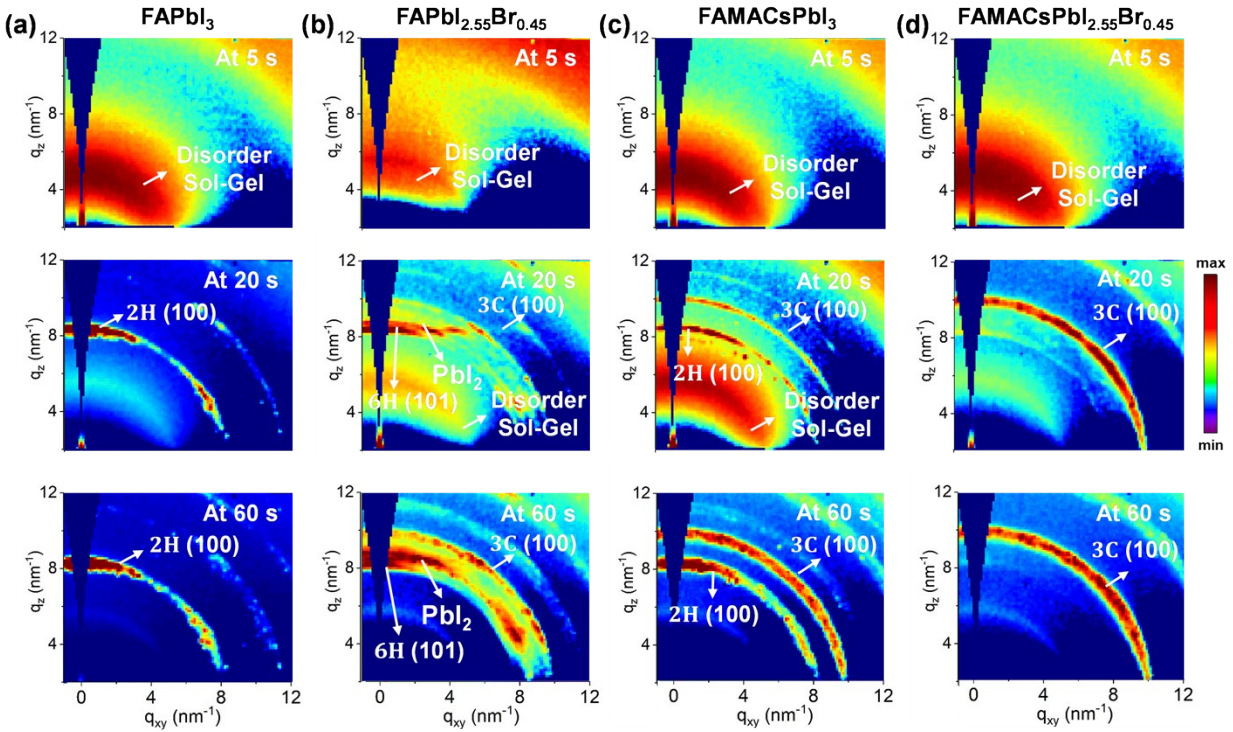


Figure S1 *In situ* representative 2D GIWAXS snapshots collected during blade coating at 120 °C of various perovskite precursor inks for (a) FAPbI_3 , (b) $\text{FAPbI}_{2.55}\text{Br}_{0.45}$, (c) $\text{FA}_{0.8}\text{MA}_{0.15}\text{Cs}_{0.05}\text{PbI}_3$, and (d) $\text{FA}_{0.8}\text{MA}_{0.15}\text{Cs}_{0.05}\text{PbI}_{2.55}\text{Br}_{0.45}$ at 5 s, 20 s, and 60 s. Scattering features associated with the disordered sol-gel phase and non-perovskite 2H phase ($q = 8.5 \text{ nm}^{-1}$) are identified along with the diffraction of PbI_2 ($q = 9.0 \text{ nm}^{-1}$) and perovskite 3C (100) phase ($q = 10.2 \text{ nm}^{-1}$).

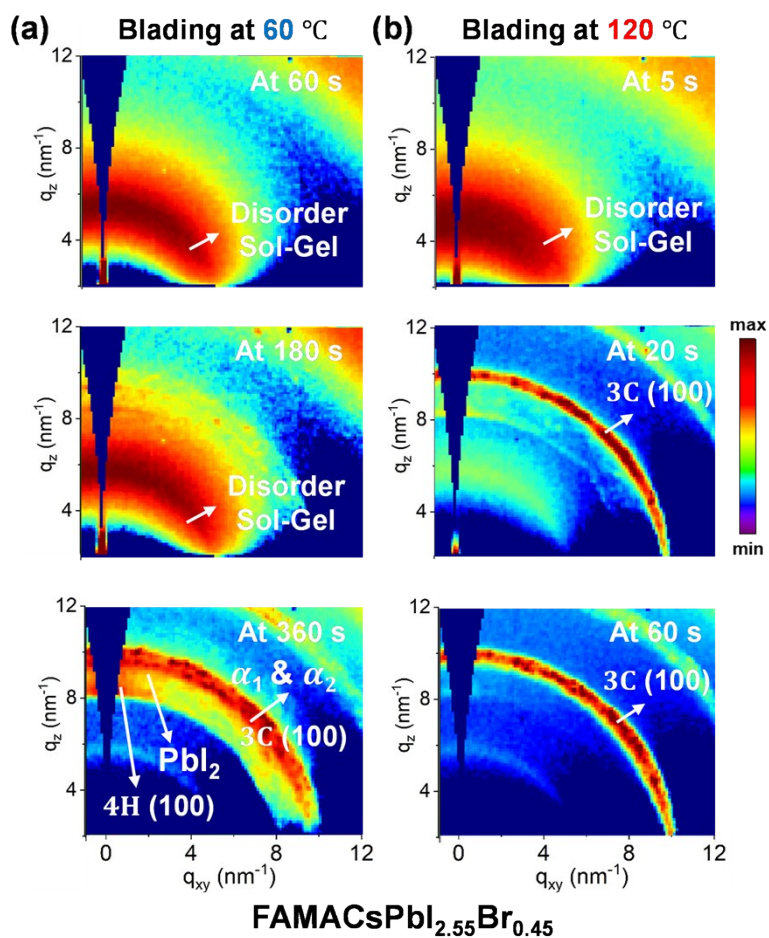


Figure S2 *In situ* representative 2D GIWAXS snapshots collected during blade coating at (a) 60 °C and (b) 120 °C of $\text{FA}_{0.8}\text{MA}_{0.15}\text{Cs}_{0.05}\text{Pb}_{2.55}\text{Br}_{0.45}$ perovskite precursor ink at different timing. Scattering features associated with the disordered sol-gel phase and non-perovskite 4H (100) phase ($q \approx 8.36 \text{ nm}^{-1}$) are identified along with the diffraction of PbI_2 ($q = 9.0 \text{ nm}^{-1}$) and perovskite 3C (100) phase ($q = 10.2 \text{ nm}^{-1}$).

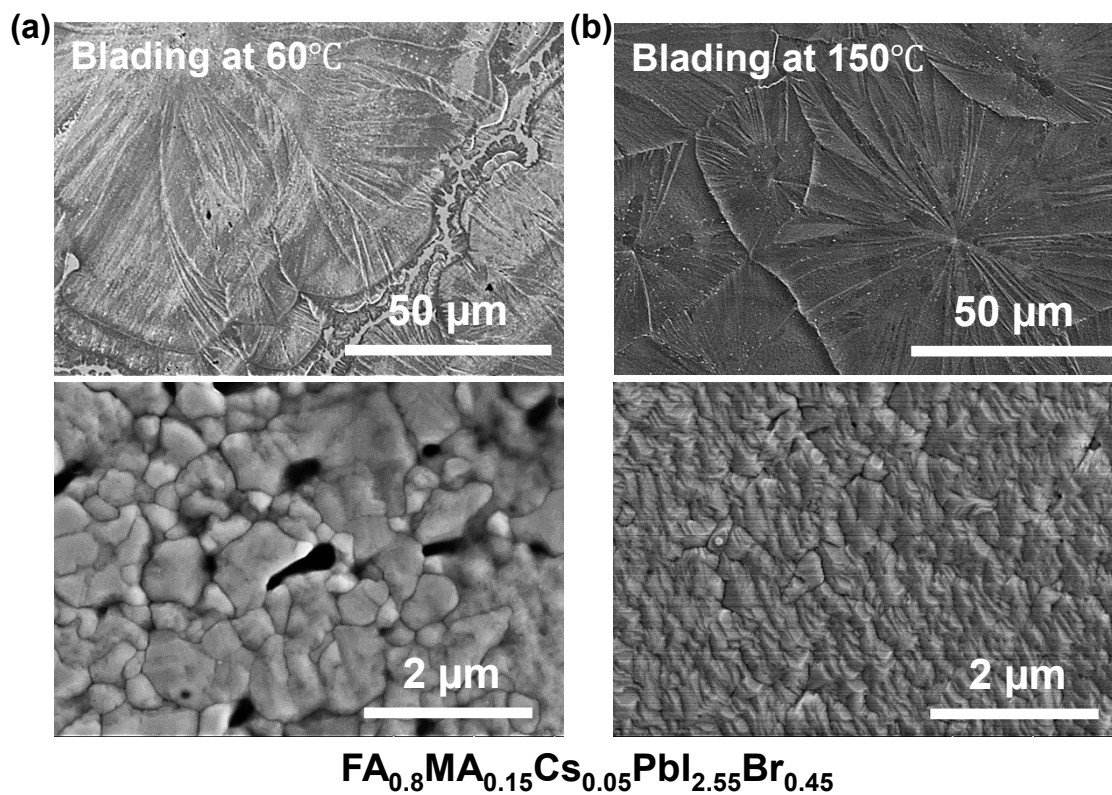
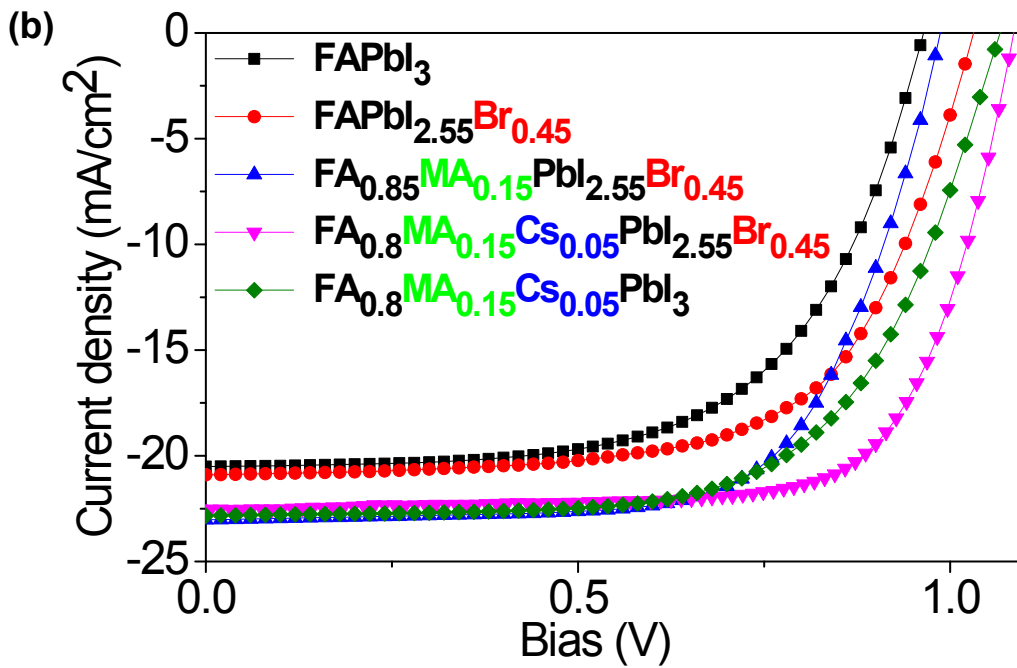
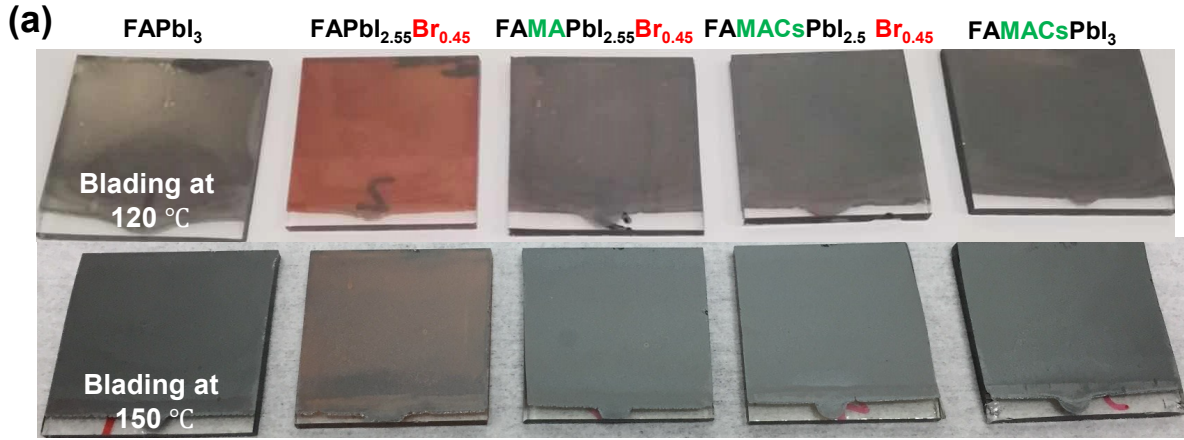


Figure S3 Top-view SEM images of $\text{FA}_{0.8}\text{MA}_{0.15}\text{Cs}_{0.05}\text{PbI}_{2.55}\text{Br}_{0.45}$ perovskite thin films using the blade-coating approach at (a) 60 °C and (b) 150 °C (top row is in smaller magnification and the bottom row is in larger magnification).



Fi

Figure S4 (a) Photographs of blade-coated perovskite thin films at 120 °C and 150 °C and (b) J - V curve of the champion device under AM1.5G illumination for each FAPbI₃, FAPbI_{2.55}Br_{0.45}, FA_{0.85}MA_{0.15}PbI_{2.55}Br_{0.45}, FA_{0.8}MA_{0.15}Cs_{0.05}PbI_{2.55}Br_{0.45}, and FA_{0.8}MA_{0.15}Cs_{0.05}PbI₃ perovskite, respectively.

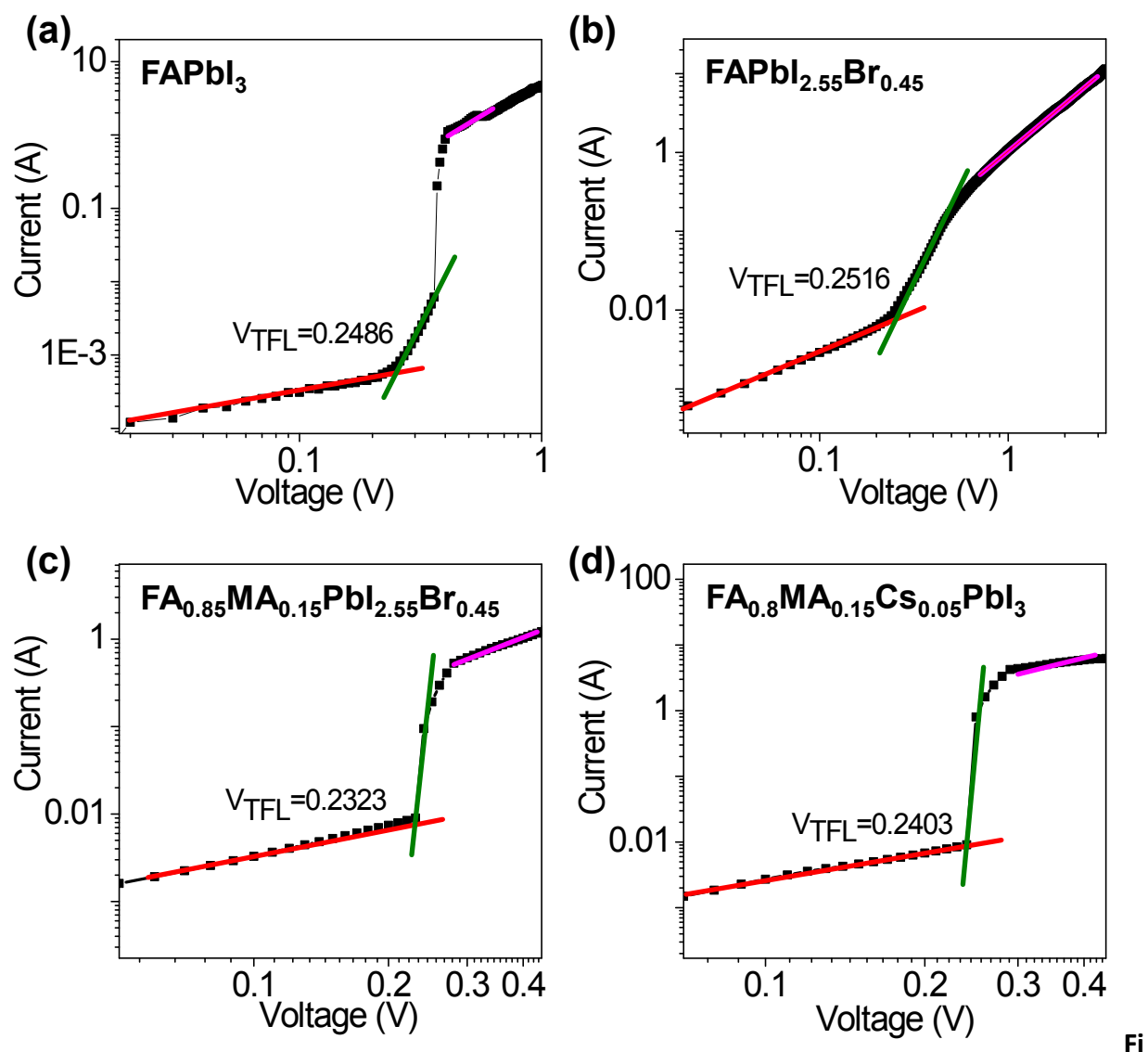


Figure S5 Dark I - V measurements of the electron-only devices displaying V_{TFL} kink point behavior for the representative (a) FAPbI_3 , (b) $\text{FAPbI}_{2.55}\text{Br}_{0.45}$, (c) $\text{FA}_{0.85}\text{MA}_{0.15}\text{PbI}_{2.55}\text{Br}_{0.45}$, and (d) $\text{FA}_{0.8}\text{MA}_{0.15}\text{Cs}_{0.05}\text{PbI}_3$. Electron-only devices (FTO/ c-TiO₂/ perovskites/ PCBM/ Ag) were fabricated to calculate the electron mobility of the devices. The dark J - V characteristics of the electron-only devices were measured by a Keithley 2400 source. The mobility is extracted by fitting the J - V curves using the Child's law given by $J = \frac{9}{8} \epsilon_0 \epsilon_r \mu_{\text{SCL}} \frac{V^2}{d^3}$, where J is the current density, V is the applied voltage, ϵ_0 is the vacuum permittivity, ϵ_r is the relative dielectric constant, and L is the thickness of the film.

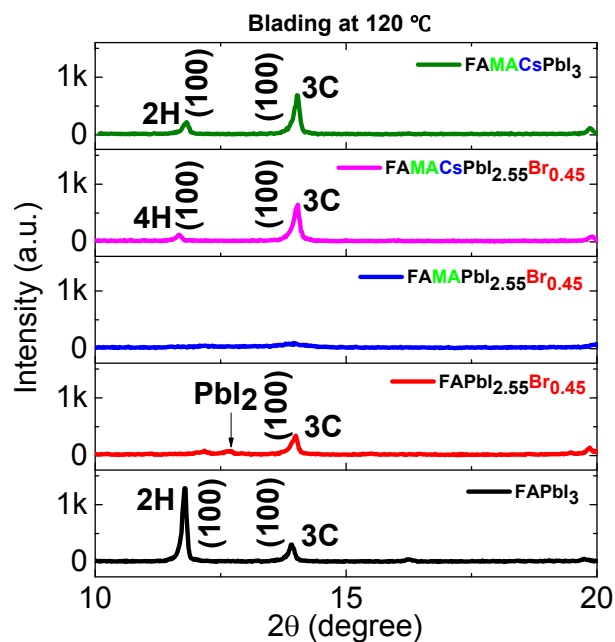


Figure S6 Comparison of FAPbI_3 , $\text{FAPbI}_{2.55}\text{Br}_{0.45}$, $\text{FAMAPbI}_{2.55}\text{Br}_{0.45}$ (i.e. $\text{FA}_{0.85}\text{MA}_{0.15}\text{PbI}_{2.55}\text{Br}_{0.45}$), FAMACsPbI_3 (i.e. $\text{FA}_{0.8}\text{MA}_{0.15}\text{Cs}_{0.05}\text{PbI}_3$) and $\text{FAMACsPbI}_{2.55}\text{Br}_{0.45}$ (i.e. $\text{FA}_{0.8}\text{MA}_{0.15}\text{Cs}_{0.05}\text{PbI}_{2.55}\text{Br}_{0.45}$) films via blade coating. XRD patterns of hybrid perovskite as-cast thin films with different precursor inks.

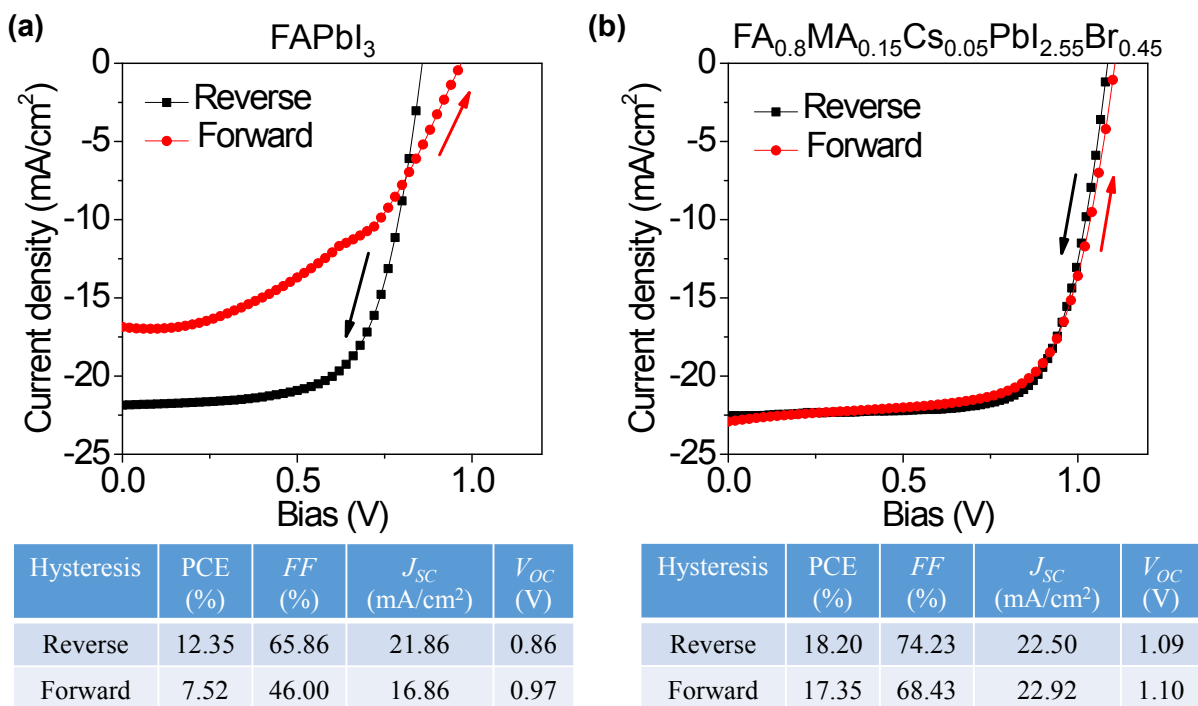


Figure S7 Representative reverse and forward scan J - V curve under AM1.5G illumination for (a) FAPbI₃ and (b) FA_{0.8}MA_{0.15}Cs_{0.05}PbI_{2.55}Br_{0.45} solar cells prepared via blade coating in ambient air at 150 °C.

References

1. Y. Zhang, P. Wang, M.-C. Tang, D. Barrit, W. Ke, J. Liu, T. Luo, Y. Liu, T. Niu, D.-M. Smilgies, Z. Yang, Z. Liu, S. Jin, M. G. Kanatzidis, A. Amassian, S. F. Liu and K. Zhao, *J. Am. Chem. Soc.*, 2019, **141**, 2684-2694.
2. J. Li, R. Munir, Y. Fan, T. Niu, Y. Liu, Y. Zhong, Z. Yang, Y. Tian, B. Liu, J. Sun, D.-M. Smilgies, S. Thoroddsen, A. Amassian, K. Zhao and S. Liu, *Joule*, 2018, **2**, 1313-1330.
3. M. Abdi-Jalebi, M. I. Dar, A. Sadhanala, S. P. Senanayak, F. Giordano, S. M. Zakeeruddin, M. Gratzel and R. H. Friend, *J. Phys. Chem. Lett.*, 2016, **7**, 3264-3269.
4. R. H. Bube, *J. Appl. Phys.*, 1962, **33**, 1733-1737.